Supporting Information

MOF-Derived Nitrogen-Doped Core-Shell Hierarchical Porous Carbon Confining Selenium for Advanced Lithium-Selenium Battery

Jian-Ping Song[a], Liang Wu[a], Wen-Da Dong[a], Chao-Fan Li[a, b], Li-Hua Chen[a*], Xin Dai[a], Chao Li[c], Hao Chen[a], Wei Zhou[a], Wen-Bei Yu[a], Zhi-Yi Hu[a, b], Jing Liu[a], Hong-En Wang[a], Yu Li[a, b*], Bao-Lian Su[a, c]

[a] State Key Laboratory of Advanced Technology for Materials Synthesis and Processing, Wuhan University of Technology, 122 Luoshi Road, 430070 Wuhan, Hubei, China.

[b] Nanostructure Research Centre (NRC), Wuhan University of Technology, 122 Luoshi Road, 430070 Wuhan, Hubei, China.

[c] Laboratory of Inorganic Materials Chemistry (CMI), University of Namur, 61 rue de Bruxelles, B-5000 Namur, Belgium.

*To whom correspondence should be addressed. Email: chenlihua@whut.edu.cn and yu.li@whut.edu.cn

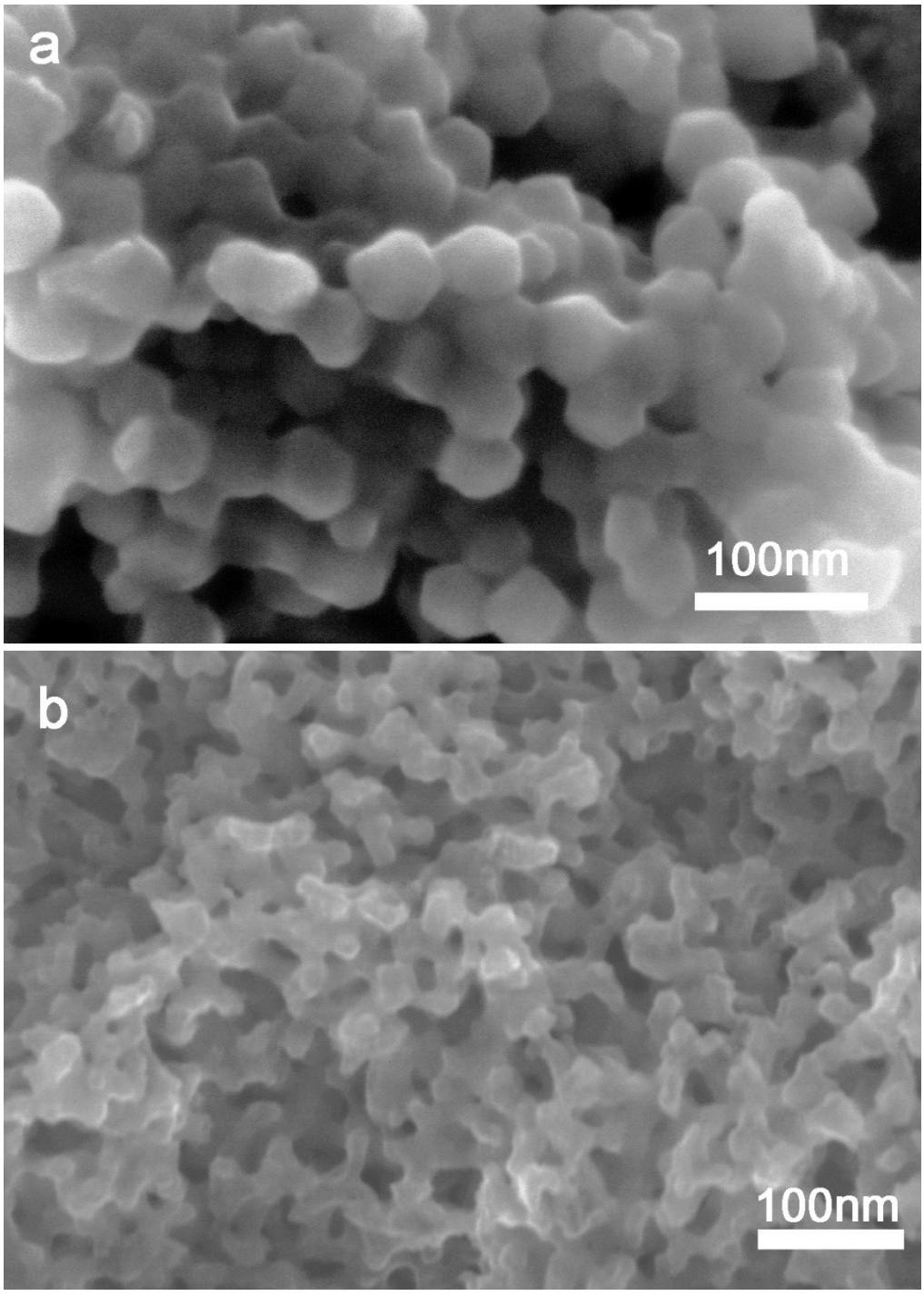

Fig. S1. SEM images of (a) the ZIF-8 nanoparticles and (b) C-ZIF-8 nanoparticles.

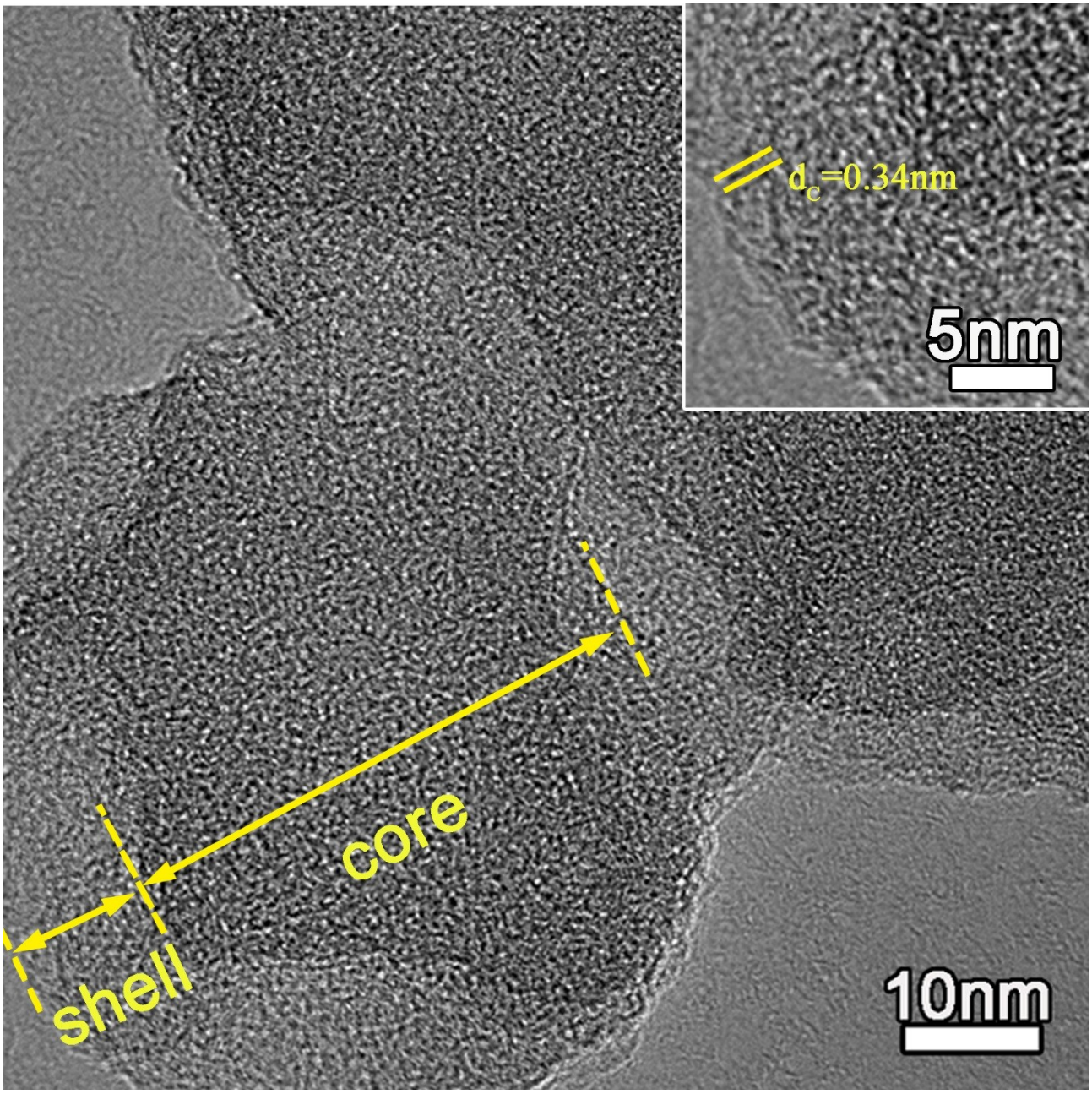

Fig. S2. HRTEM image of N-CSHPC-II, clearly showing the graphic layer in the hierarchical core-shell porous structure.

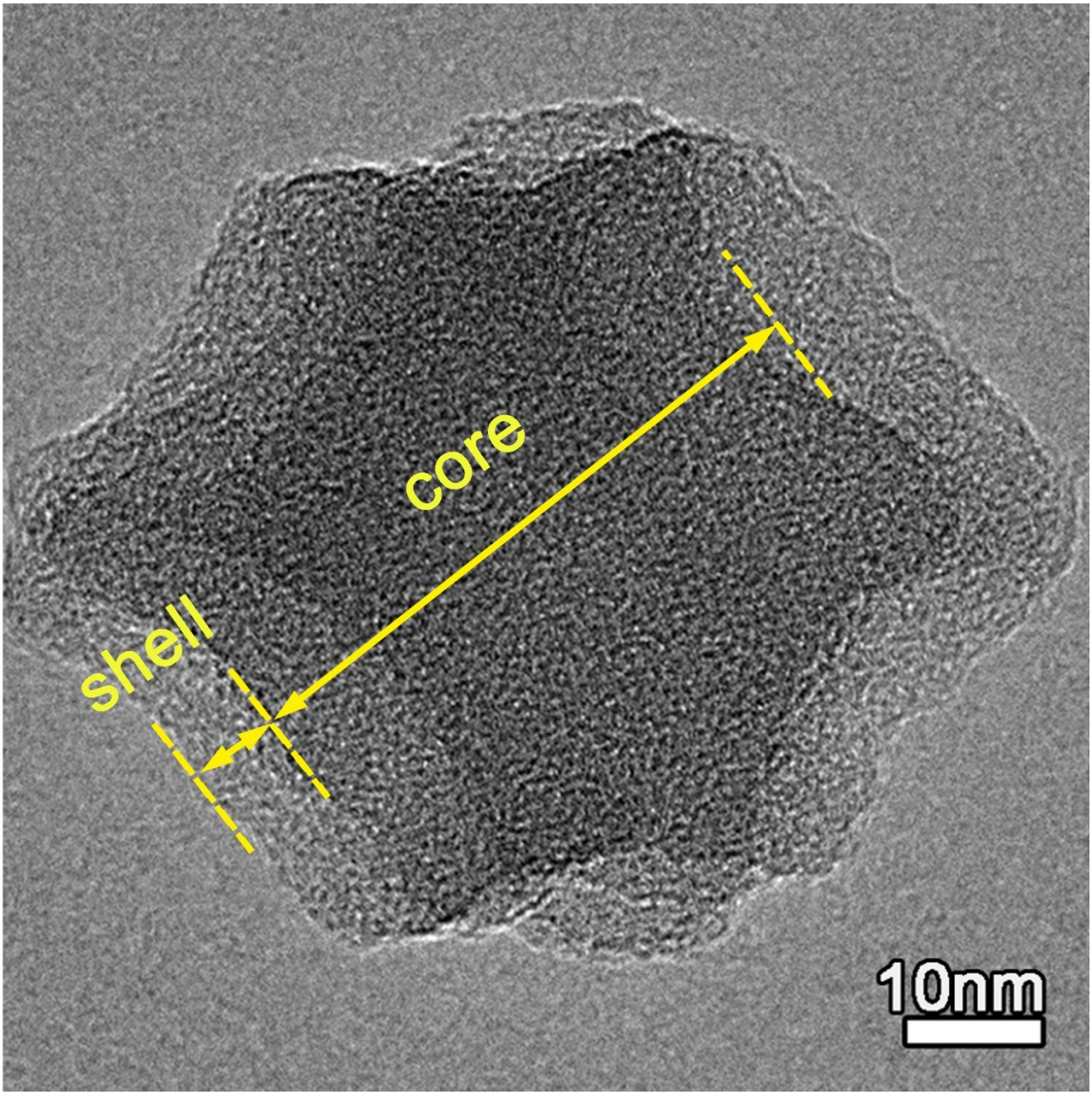

Fig. S3. HRTEM image of Se/N-CSHPC-II, showing that most of the pores inside the core cannot be observed.

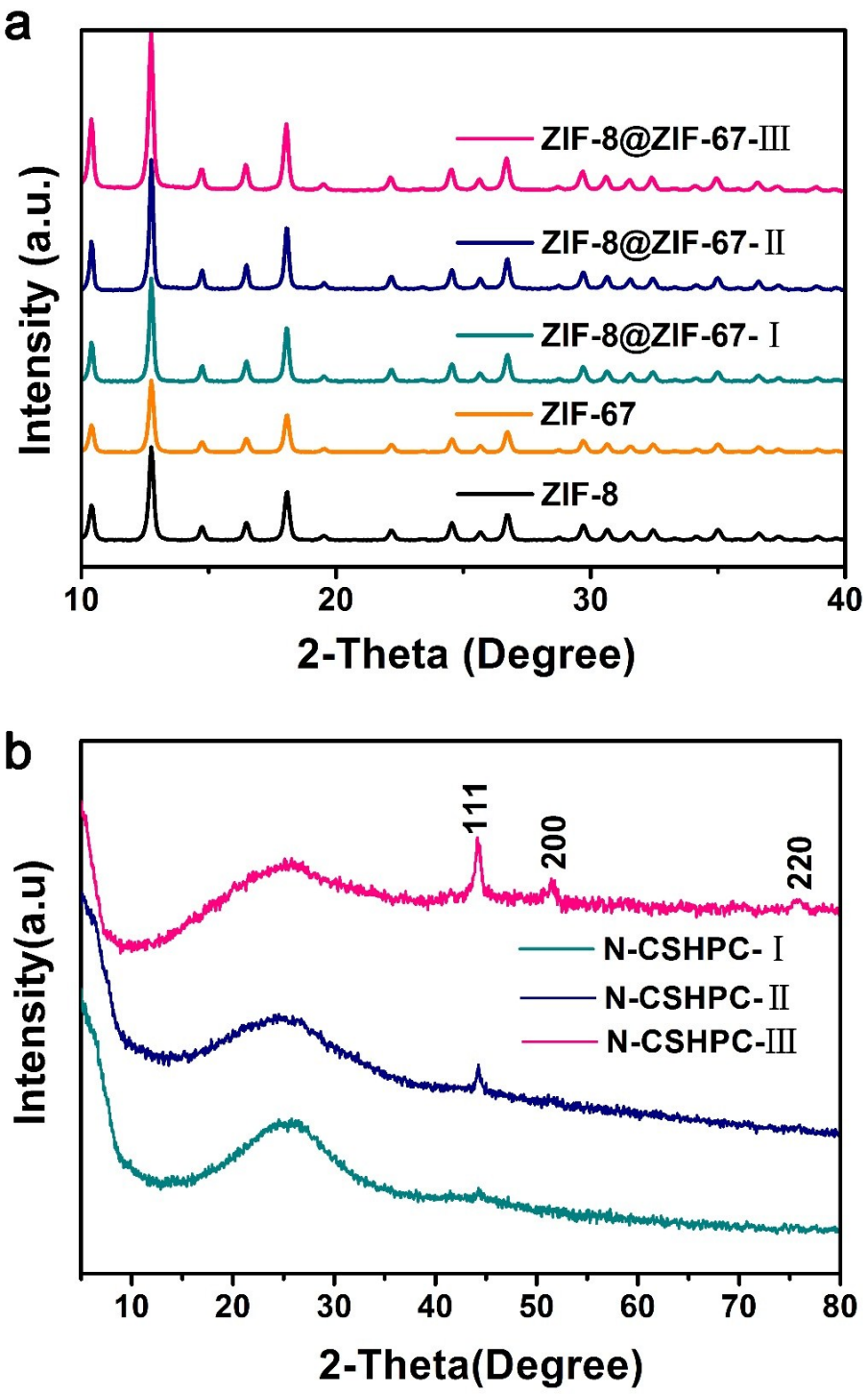

Fig. S4. XRD patterns of (a) ZIF-8, ZIF-67, ZIF-8@ZIF-67-I , ZIF-8@ZIF-67-II and ZIF-8@ZIF-67-III , and (b) N-CSHPC.

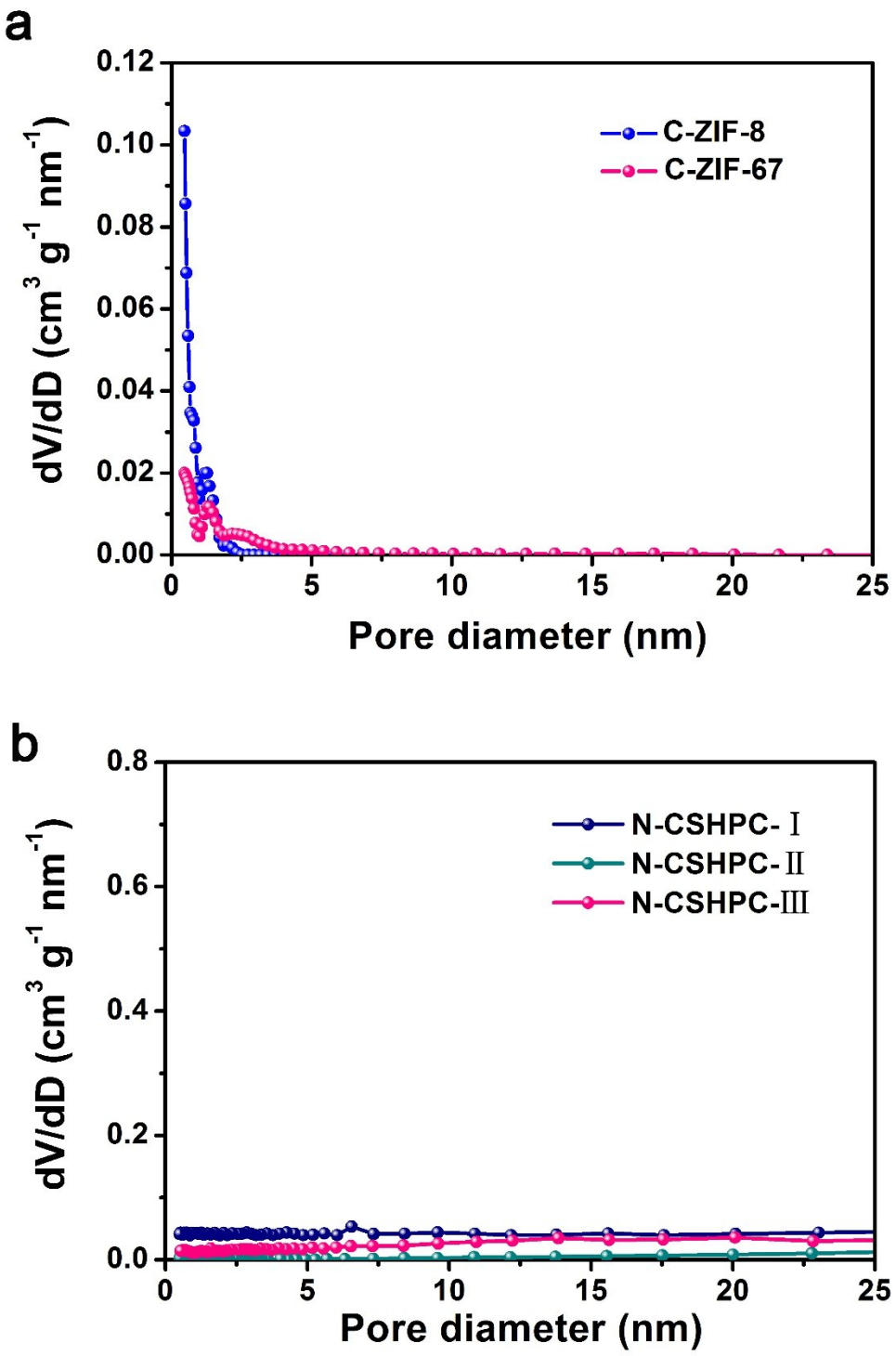

Fig. S5. (a) Pore size distribution of C-ZIF-8 and C-ZIF-67 and (b) Pore volume distribution of Se/N-CSHPC.

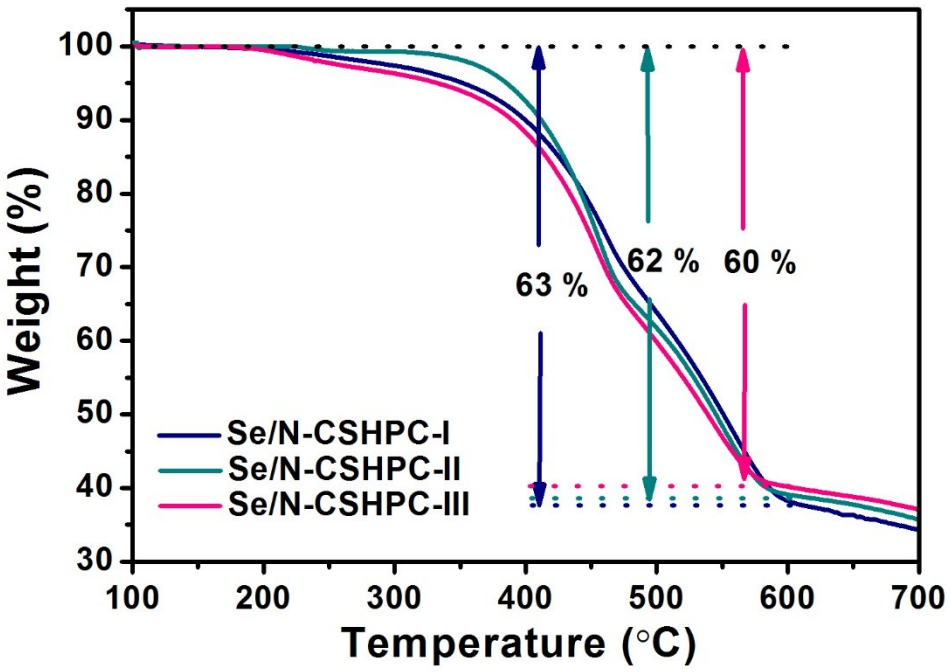

Fig. S6. TG curve of Se/N-CSHPC.

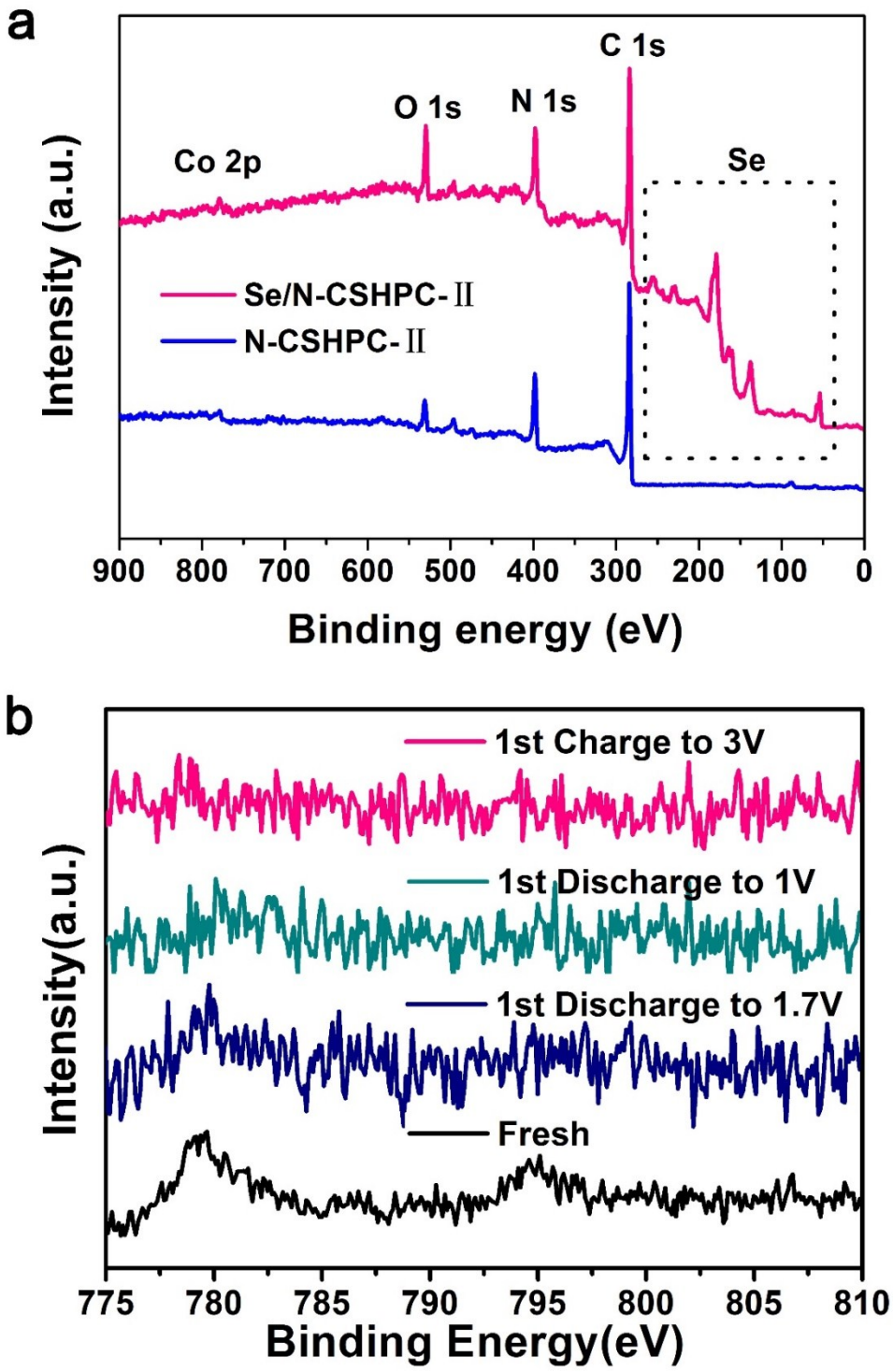

Fig. S7. (a) XPS survey scan of N-CSHPC-II and Se/N-CSHPC-II, (b) XPS survey scan of fresh electrode material, 1st discharge to 1.7V, 1V, and 1st charge to 3V.

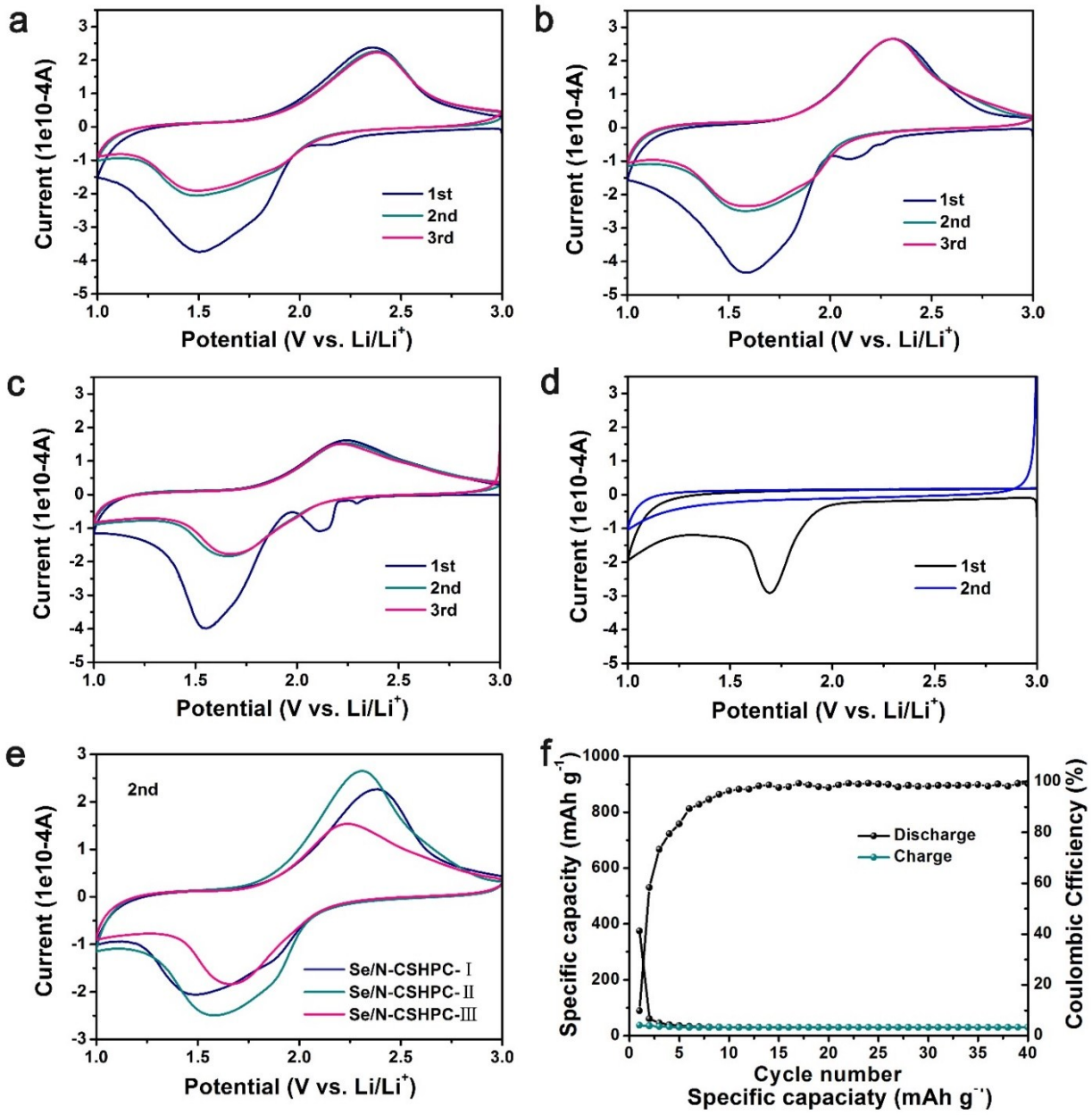

Fig. S8. (a) CV curves of Se/N-CSHPC-I, (b) Se/N-CSHPC-II, and (c) Se/N-CSHPC-III at a sweep rate of 0.2 mV s-1. (d) CV curves of N-CSHPC-II. (e) 2nd CV curves of Se/N-CSHPC. (f) Typical voltage profiles of N-CSHPC-II.

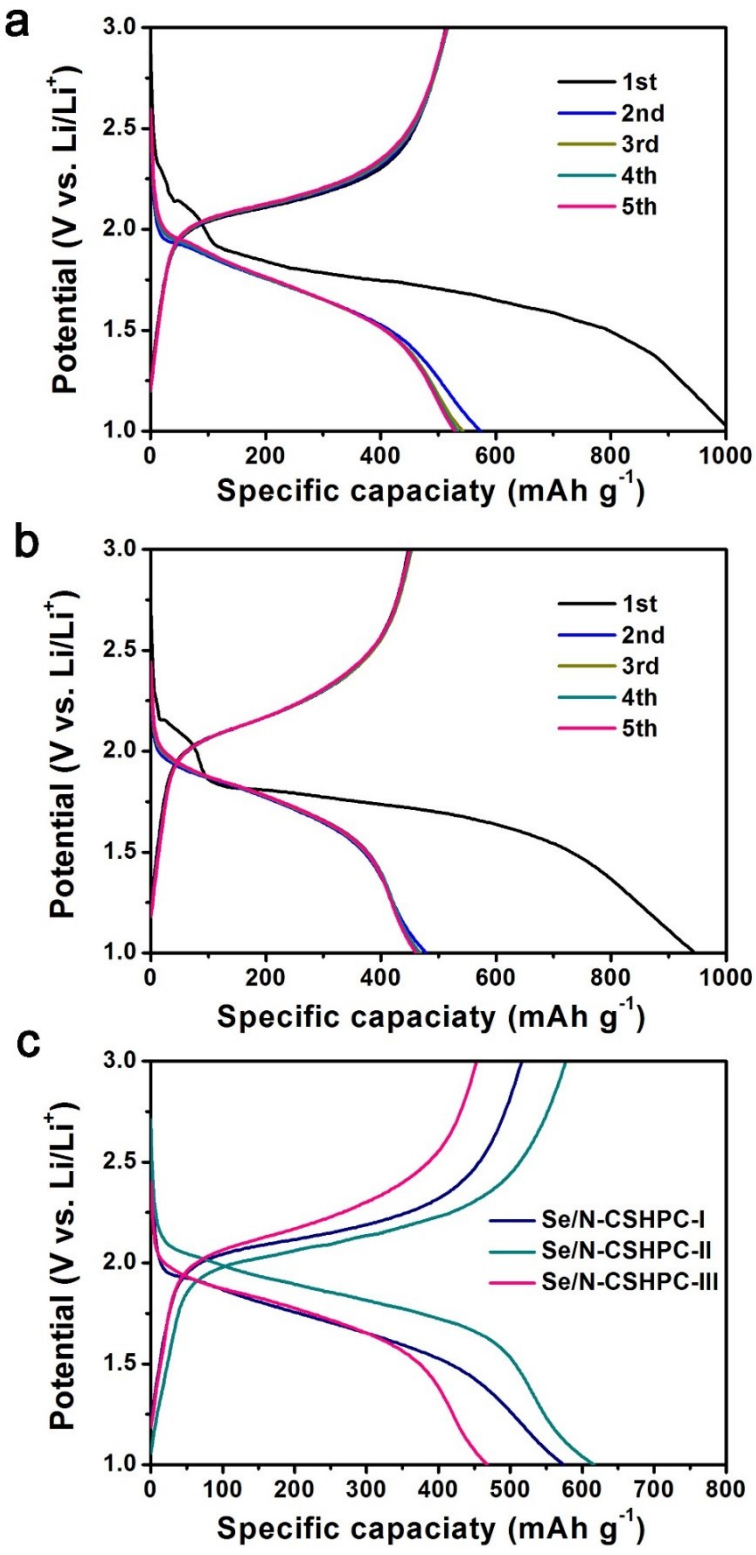

Fig. S9. (a)Typical voltage profiles of Se/N-CSHPC-I and (b) Se/N-CSHPC-III for the first five cycles. (c) 2nd typical voltage profiles of Se/N-CSHPC.

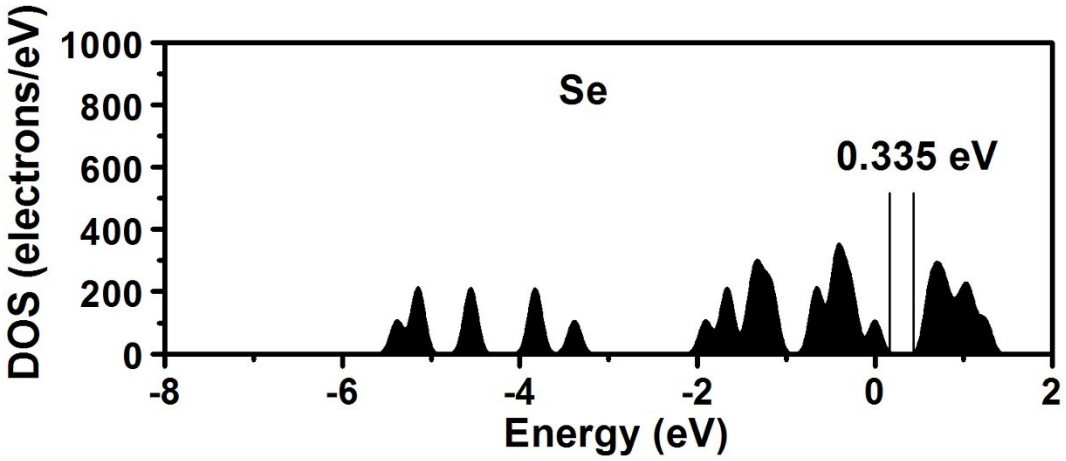

Figure S10. DOS spectrum of Se.

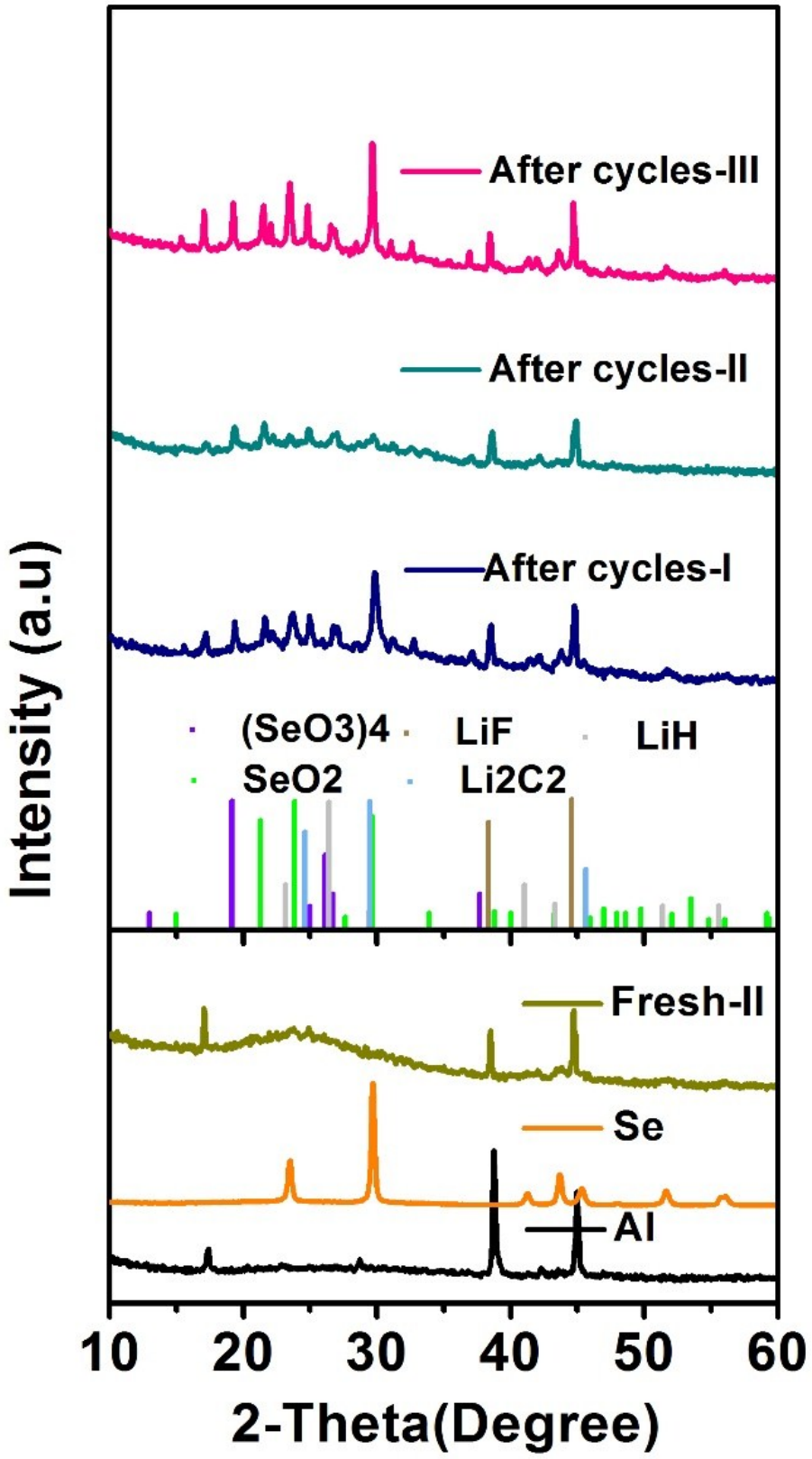

Figure S11. XRD patterns of Se/N-CSHPC before and after 200 cycles.

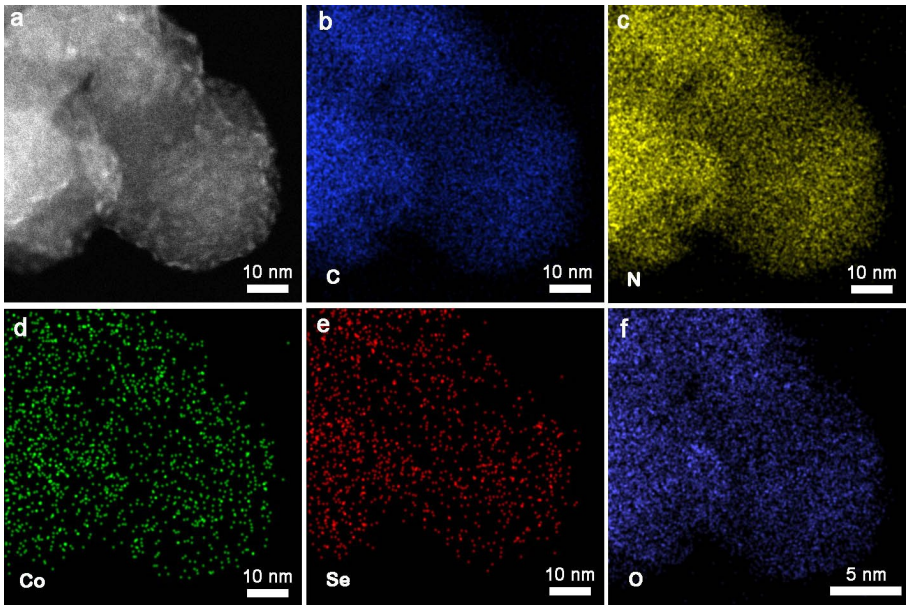

Fig. S12. (a) A typical HAADF-STEM image and (b-e) the corresponding EDX elemental mappings of Se/N-CSHPC-II after 200 cycles at 1C.

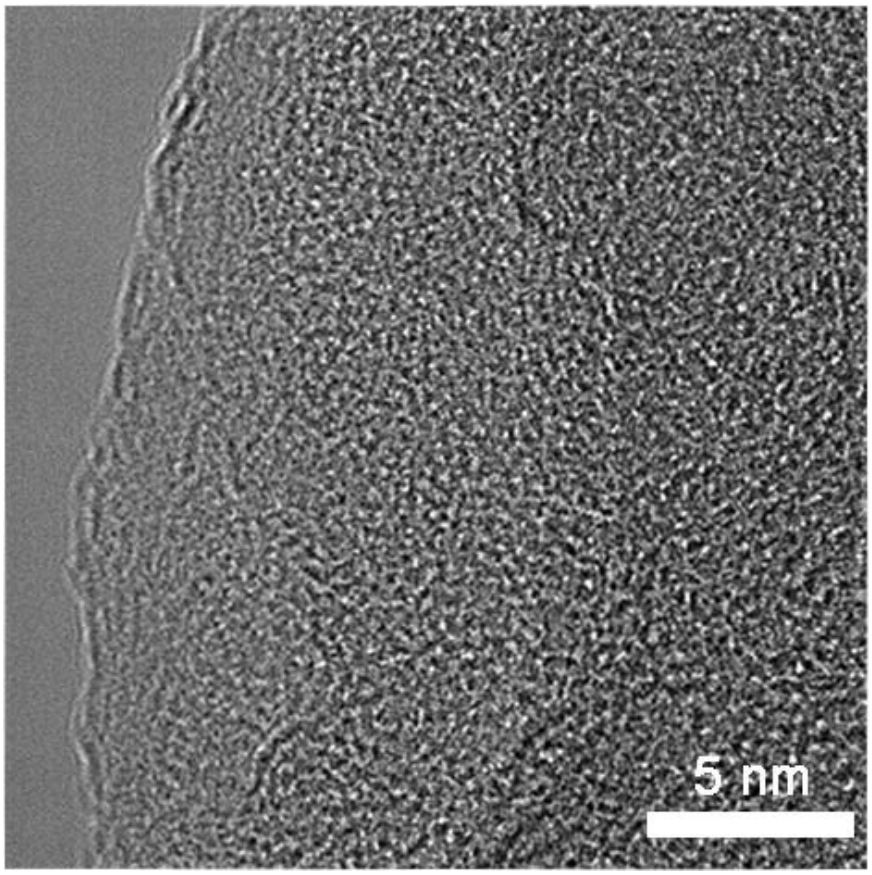

Fig. S13. A typical HRTEM image of Se/N-CSHPC-II after 200 cycles at 1C.

Table S1. The Energy efficiency of Se/N-CSHPC at 1st, 100th and 200th cycle.

Items	Se/N-CSHPC-I	Se/N-CSHPC-II	Se/N-CSHPC-III
1st Charging energy (mWh)	0.718	0.781	0.608
1st Discharge energy (mWh)	1.035	1.117	0.905
1st Energy efficiency (%)	144.2	143.0	148.8
100th Charging energy (mWh)	0.635	0.692	0.587
100th Discharge energy (mWh)	0.546	0.598	0.501
100th Energy efficiency (%)	86.0	86.4	85.3
200th Charging energy (mWh)	0.617	0.666	0.549
200th Discharge energy (mWh)	0.521	0.574	0.462
200th Energy efficiency (%)	84.4	86.2	84.1